IEEE Access
Multidisciplinary | Rapid Review | Open Access Journal

Received May 13, 2020, accepted May 22, 2020, date of publication May 29, 2020, date of current version June 11, 2020.

Digital Object Identifier 10.1109/ACCESS.2020.2998494

Interference Management in Ultra-Dense 5G Networks With Excessive Drone Usage

MUHAMMAD SAJID HAROON[1], (Graduate Student Member, IEEE), FAZAL MUHAMMAD[2], GHULAM ABBAS[3], (Senior Member, IEEE), ZIAUL HAQ ABBAS[4], AHMAD KAMAL HASSAN[4], MUHAMMAD WAQAS[3], AND SUNGHWAN KIM[5], (Member, IEEE)

[1]Telecommunications and Networking (TeleCoN) Research Laboratory, Ghulam Ishaq Khan Institute of Engineering Sciences and Technology, Swabi 23640, Pakistan
[2]Department of Electrical Engineering, City University of Science and Information Technology, Peshawar 2500, Pakistan
[3]Faculty of Computer Science and Engineering, Ghulam Ishaq Khan Institute of Engineering Sciences and Technology, Swabi 23640, Pakistan
[4]Faculty of Electrical Engineering, Ghulam Ishaq Khan Institute of Engineering Sciences and Technology, Swabi 23640, Pakistan
[5]School of Electrical Engineering, University of Ulsan, Ulsan 44610, South Korea

Corresponding author: Sunghwan Kim (sungkim@ulsan.ac.kr)

This work was supported by the National Research Foundation of Korea through the Research Program under Grant NRF-2019R1A2C1005920.

ABSTRACT In fifth generation (5G) networks, the densification of small base stations in the coverage region of macro base station (MBS) leads to significant inter-cell interference (ICI). Similarly, drones (a.k.a. unmanned aerial vehicles) have a diverse scope in multifarious 5G assisted applications and, therefore, cause considerable drones interference (DI) as a result of excessive drone usage. This paper investigates the bottleneck uplink (UL) coverage performance of the MBS edge users in the presence of ICI and DI. To mitigate both ICI and DI, we use an efficient resource allocation scheme known as reverse frequency allocation (RFA). Moreover, we use decoupled association (DeCA) in place of coupled association to further improve UL signal-to-interference ratio. The results depict that RFA in conjunction with DeCA overpass all other techniques in terms of improved UL coverage performance because of effective DI and ICI mitigation.

INDEX TERMS Coverage probability, coupled association, decoupled association, heterogeneous cellular networks, interference mitigation, reverse frequency allocation.

I. INTRODUCTION

A. MOTIVATION

In fifth-generation (5G) networks, ultra-dense deployment of small base stations (SBSs) in the macro base station (MBS)' coverage region, high MBS transmit power, and aggressive frequency reuse lead to significant inter-cell interference (ICI) [1]–[4]. Meanwhile, unmanned aerial vehicles, popularly known as drones, are expected to be used excessively for 5G assisted applications because of their higher maneuverability, hovering, ease of deployment, and lower maintenance and operating costs [5], [6]. The prominent 5G applications of drones include mineral exploration, precision agriculture, smart logistics, air surveillance, disaster assistance, and emergency healthcare [7], [8]. Such applications demand for an excessive use of drones assisted by 5G networks. However, such excessive drone usage (EDU) leads to additional traffic load in conjunction with users' traffic load and, hence, causes significant drones interference (DI). In this paper, we explore the effect of DI and ICI on the bottleneck uplink (UL) communication of MBS coverage edge users (M-EUs). Here, the bottleneck UL communication indicates the limitations in UL communications, i.e., (i) lower UL transmit power by user equipment (UE), which leads to lower UL signal-to-interference ratio (SIR), and (ii) limited available power in battery-operated UEs [9], [10].

In two-tier heterogeneous cellular networks (HetNets), coupled association (CA) is often considered, where a user equipment (UE) associates with the same base station (BS) both in downlink (DL) and UL following the maximum received power (MRP) association rule [11], [12]. CA is typically followed when the UEs are closer to the serving BS. However, the M-EUs following CA experience lower signal-to-interference ratio (SIR) because of their longer

The associate editor coordinating the review of this manuscript and approving it for publication was Barbara Masini.

distances from the BS [13], [14]. Therefore, decoupled association (DeCA) has attracted considerable attention, where a user associates in UL and DL directions with different tiers of BSs [15]. By using DeCA, UL SIR of M-EUs is significantly increased because of nearest SBS association [15].

In the state-of-the-art, different interference management schemes, such as fractional frequency reuse (FFR) [16] and soft frequency reuse (SFR) [17], have been studied. The SFR scheme achieves better spectral efficiency as a result of frequency reuse, while FFR leads to lower interference due to partitioning of total available bandwidth [18], [19]. Another proactive resource allocation scheme available in the state-of-the-art is reverse frequency allocation (RFA) [20]–[22]. In RFA, the complete bandwidth is made available to both MBS and SBS in a cell. Thus, RFA is spectrally more efficient as compared with both FFR and SFR. Therefore, we employ RFA with DeCA to alleviate ICI and DI (see Sec. II-B2 for details on RFA).

B. RELATED WORK

In [23], the authors examine the effects of users and device mobility in device-to-device (D2D) and drone-assisted mission-critical machine-type communications. Their results show that D2D links and drone-assisted access lead to 40% improvements in link availability and reliability on top of the cellular-only baseline. The work in [24] investigates the security challenges posed by drones to sensitive installations. The paper also highlights the importance of drone monitoring, which can help to avoid damages to sensitive installations. Diverse drone platform applications and challenges in the network infrastructure are discussed in [25]. Their study highlights the significance of using drones in heterogeneous networks to improve the network capacity and coverage. The work in [26] investigates the use of drones mounted miniaturized BSs to serve the network mobile users. The authors propose that the drones move continuously within the cell. Therefore, their proposed setup reduces the distance between the BS and the UEs and, hence, improves spectral efficiency of the network. The simulation results in [26] indicate that their proposed model leads to improved spectral efficiency as compared with the scenario where drones hover over fixed locations. In [27], the authors evaluate the usage of drones in conventional terrestrial cellular networks. They investigate DL spectral efficiency of the network with optimal altitude and intensity of drones. Their results show that drones' usage provides improved DL spectral efficiency for conventional terrestrial cellular networks. Similarly, the authors in [28] evaluate drones' usage in multiple-input multiple-output (MIMO) and non-orthogonal multiple access assisted networks while utilizing stochastic geometry framework. They derive outage probability expressions for proposed setup. Their results show that rate and coverage of far users rely on power allocation factors.

RFA along with CA and DeCA are considered in [29]. The authors derive DL coverage probability expressions for their proposed setup. Their results show that RFA along with DeCA overpass other techniques with respect to coverage performance in the DL. In [30], the authors investigate interference mitigation and resource management while employing D2D communications. Moreover, the authors employ DeCA and FFR in conjunction with their proposed setup. Their results show that their proposed model significantly abates the interference.

The work in [31] considers RFA in non-uniform HetNets. It is assumed that the SBSs located near MBS are muted while SBSs remain active in the MBS edge area. The results indicate that non-uniform HetNets with RFA lead to improved UL coverage. The work in [32] proposes modified RFA, which leads to significant coverage improvement as a result of reduced interference.

This work is different from the state-of-the-art as follow:

1) The works in [23]–[28] discuss various application scenarios of drone usage. However, they lack the analysis of DI because of 5G assisted EDU. Therefore, in this paper, we investigate both DI and ICI that affect the bottleneck UL SIR of M-EUs.
2) The works in [29]–[32] analyze DL coverage in the presence of ICI, however, in this paper, we investigate UL coverage performance in the presence of ICI and DI.

C. CONTRIBUTIONS

In this paper, we investigate DI due to EDU for 5G assisted applications and ICI due to multi-tier deployment. The coverage region of MBS is split into non-intersecting regions, i.e., center region, A_{M}^{c}, and outer region, A_{M}^{o}, with radii d_1 and d_2, respectively (see Fig. 1). The analysis is performed on typical user, ν, located in A_{M}^{o}. The main contributions of this paper are listed as follows:

1) Investigation of bottleneck M-EUs' UL coverage performance in the presence of both DI and ICI.
2) Mitigation of DI and ICI by utilizing RFA along with DeCA and, hence, improving UL SIR of the M-EUs.
3) Derivations of the UL coverage probabilities for the following network scenarios for $\nu \in A_{\mathrm{M}}^{o}$: (i) RFA, CA, and EDU, and (ii) RFA, DeCA, and EDU.
4) The results depict 16% UL coverage improvement as observed at SIR threshold, $\gamma_{\mathrm{M}}, = -10$ dB by DeCA with RFA employment in contrast to CA with RFA employment. Moreover, at $\gamma_{\mathrm{M}} = -10$ dB and drones density, $\rho_{\mathrm{D}}, = 50$, DeCA and RFA cause 8% UL coverage improvement in comparison with CA and RFA. Furthermore, increasing ρ_{D} from 100 to 150 at $\gamma_{\mathrm{M}} = -10$ dB leads to 15% UL coverage degradation because of significant DI.

In the results, we show that an increase in ρ_{D} causes significant DI and consequently lowers the UL coverage. Moreover, the results indicate that RFA with DeCA produces improved UL coverage as opposed to CA with RFA.

D. PAPER ORGANIZATION

The rest of the paper is organized as follows. After presenting the system model in Section II, UL coverage probabilities are

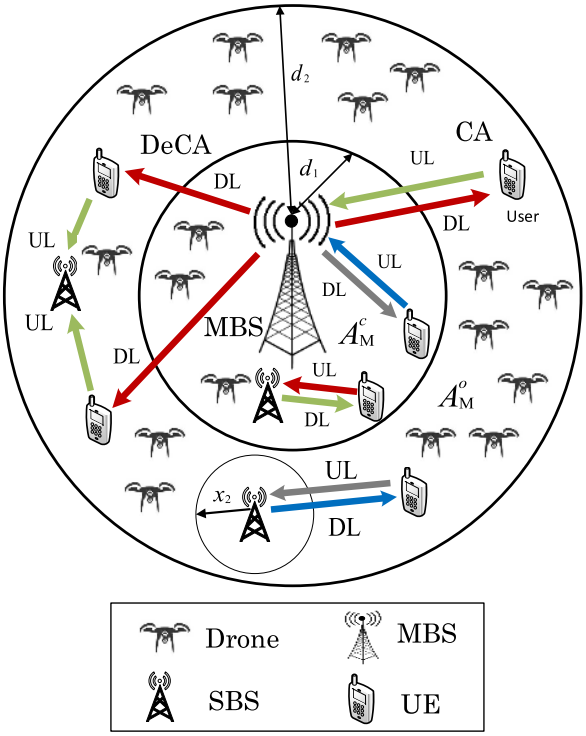

FIGURE 1. A multi-tier HetNet deployment model with EDU, RFA and DeCA. A_M^c and A_M^o denote the center and outer regions of MSB, respectively.

TABLE 1. Notation summary.

Notation	Description
$'$	Decoupled association
$''$	Coupled association
ν	Typical user
α	Path loss exponent
$\|h\|$	Power gain of Rayleigh fading
ζ_1	Ratio of $P_{t,S}^{DL}$ and $P_{t,\nu}^{UL}$
ζ_2	Ratio of $P_{t,D}^{DL}$ and $P_{t,\nu}^{UL}$
ϕ_M, ϕ_S, ϕ_D	IHPPPs of MBSs, SBSs, and drones, respectively
γ_M, γ_S	SIR thresholds for MBSs and SBSs, respectively
d_1, d_2	Radii of A_M^c and A_M^o, respectively
ρ_M, ρ_S, ρ_D	Densities of MBSs, SBSs, and drones, respectively
r_l, r_k, r_j	Distances from MBSs, SBSs, and drones, $\forall\, l \in \{\phi_M\}, k \in \{\phi_S\}$, and $j \in \{\phi_j\}$

derived in Section III. Numerical and simulation results with discussion are presented in Section IV. Finally, Section V concludes our work and presents future directions. The notations used in this paper are listed in Table 1.

II. SYSTEM MODEL

This section presents the proposed network layout with DI due to EDU for 5G assisted applications and ICI due to multi-tier deployment. Moreover, DeCA and RFA are employed to abate ICI and DI. Furthermore, in this section, we develop mathematical preliminaries that will be used for the UL coverage analysis afterwards.

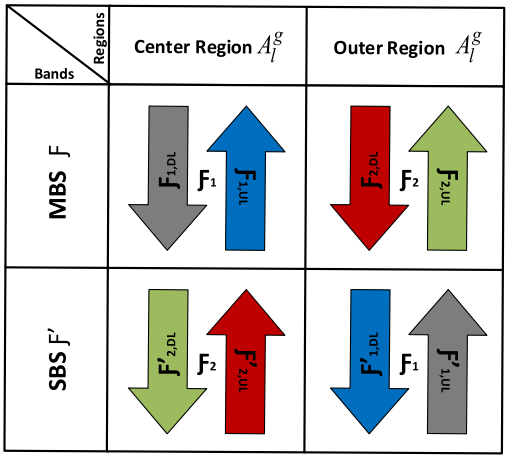

FIGURE 2. Frequency allocation in the two-tier HetNets via RFA.

A. NETWORK LAYOUT WITH ASSUMPTIONS

In this paper, we consider a two-tier HetNet, comprising of MBSs, SBSs, and drones with densities ρ_M, ρ_S, and ρ_D, respectively. MBSs, SBSs, UEs, and drones are deployed using independent homogeneous Poisson point processes (IHPPPs), i.e., ϕ_M, ϕ_S, ϕ_u, and ϕ_D, respectively, as shown in Fig. 1. This work considers frequency division duplex (FDD) systems, where different channels are used for UL and DL as indicated in Fig. 1 and Fig. 2. This work can be extended to incorporate time division duplex (TDD) systems, where the same frequency is used for both UL and DL directions in different time slots [33]. In contrast to FDD systems, TDD system with DeCA leads to lower interference at the cost of increased synchronization signaling [34]. We investigate DI resulting from EDU and ICI because of multi-tier deployment. To mitigate DI and ICI, we use RFA with DeCA as opposed to RFA with CA. Interference is considered to be the dominant performance limiting factor and, thus, noise is ignored. The analysis is performed on ν located at the origin by using the Slivnyak Theorem which retains and simplifies the statistical properties of IHPPPs [21], [35]. This work assumes Rayleigh fading for tractability in SIR analysis using Laplace transform (LT) [36]. In particular, $|h|$ models Rayleigh fading, which is independent and exponentially distributed with unit mean, i.e., $|h| \sim \exp(1)$ [37].

B. OVERVIEW OF SCHEMES

Here, we give a brief overview of the schemes used in this paper from the system model perspective.

1) COUPLED AND DECOUPLED ASSOCIATIONS

According to CA, ν associates both in UL and DL with the identical tier ω_1 following the DL association rule (see

Definition 1 for the DL association rule) [15]. However, according to DeCA, v associates in the DL with tier ω_1 based on the DL association rule and with another tier ω_2 in the UL based on UL association rule (see **Definition** 2 for the UL association rule [29]). Therefore, by following DeCA in our proposed model, v associates in the DL with MBS following MRP, and with the SBS in the UL based path loss model.

Definition 1: (DL association rule). In the DL association rule, a user connects in the DL with tier ω_1 following MRP scheme [12]. Association with ω_1 can be expressed as

$$\omega_1 = arg\ \max_{i\in(M,S)} P_{t,i}^{DL} r_{i,v}^{-\alpha}. \tag{1}$$

Here, $P_{t,i}^{DL}$ denotes the transmit power of BS in DL, r indicate the distance between v and associated BS, and α indicates the path loss exponent.

Definition 2: (UL association rule). According to UL association rule, a user associates in the UL with tier ω_2 based on path loss, i.e., $r^{-\alpha}$ [29]. The association with ω_2 can be expressed as

$$\omega_2 = arg \max_{i\in(M,S)} r_i^{-\alpha}. \tag{2}$$

2) REVERSE FREQUENCY ALLOCATION

In HetNets high throughput is obtained by frequency reuse. This, however, leads to severe ICI because of co-channel interference. Therefore, there is a need for effective interference management scheme. Hence, we use RFA (an FDD system) in conjunctions with DeCA to increase spectral efficiency due to lower interference. In RFA, the total available frequency band, $\mathcal{F}$, is split into two sub-bands, i.e., $\mathcal{F}_1$ and $\mathcal{F}_2$, such that $\mathcal{F} = \bigcup_{j\in1,2} \mathcal{F}_j$. Here, frequency sub-bands of MBS, i.e., $\mathcal{F}_1$ and $\mathcal{F}_2$ are used in A_{M}^c and A_{M}^o, respectively, as shown in Fig. 2. The sub-bands $\mathcal{F}_1$ and $\mathcal{F}_2$ are further divided into UL and DL sub-carriers of the MBS and are denoted as $\mathcal{F}_1 = \mathcal{F}_{1,\mathrm{UL}} + \mathcal{F}_{1,\mathrm{DL}}$ and $\mathcal{F}_2 = \mathcal{F}_{2,\mathrm{UL}} + \mathcal{F}_{2,\mathrm{DL}}$, in A_{M}^c and A_{M}^o, respectively [4]. The UL and DL sub-carriers in $\mathcal{F}_1$ and $\mathcal{F}_2$ of MBS are used as the frequency sub-carriers in $\mathcal{F}_1'$ and $\mathcal{F}_2'$ for the SBS in reverse direction, i.e., DL and UL transmissions with corresponding alternate regions A_{M}^o and A_{M}^c, respectively [4], [11]. Similarly, the UL and DL sub-carriers of the SBS in A_{M}^c and A_{M}^o are denoted as $\mathcal{F}_2 = \mathcal{F}_{2,\mathrm{UL}}' + \mathcal{F}_{2,\mathrm{DL}}'$ and $\mathcal{F}_1' = \mathcal{F}_{1,\mathrm{UL}}' + \mathcal{F}_{1,\mathrm{DL}}'$, respectively. RFA provides improved UL coverage because of effective ICI mitigation [20], [29].

III. ANALYSIS OF COVERAGE PROBABILITY

In this section, we derive UL coverage probability expressions for: (i) EDU, RFA, and CA, (see Sec. III-A), and (ii) EDU, RFA, and DeCA (see Sec. III-B).

A. UL COVERAGE PROBABILITY WITH CA

The UL coverage probability given that $v \in A_{\mathrm{M}}^o$, $P_{A_{\mathrm{M}}^o}^{\mathrm{UL}''}(\gamma_{\mathrm{M}})$, while assuming EDU, RFA, and CA, can be written as [20]

$$P_{A_{\mathrm{M}}^o}^{\mathrm{UL}''}(\gamma_{\mathrm{M}}) = P\left(\mathrm{SIR}_{\mathrm{M}}^{\mathrm{UL}} > \gamma_{\mathrm{M}}\right). \tag{3}$$

Here, $\mathrm{SIR}_{\mathrm{M}}^{\mathrm{UL}}$ is the UL received SIR by MBS and γ_{M} is the SIR threshold of MBS. Because of RFA, the UL interference received is the union of MBS-tier UL interference in A_{M}^c, $I_{\phi_{\mathrm{M}},A_{\mathrm{M}}^c}^{\mathrm{UL}}$, SBS-tier DL interference in A_{M}^o, $I_{\phi_{\mathrm{S}},A_{\mathrm{M}}^o}^{\mathrm{DL}}$, and the interference from EDU, $I_{\phi_{\mathrm{D}},A_{\mathrm{M}}^c}^{\mathrm{DL}}$. Therefore, $\mathrm{SIR}_{\mathrm{M}}^{\mathrm{UL}}$ from (3) can be rewritten as

$$\mathrm{SIR}_{\mathrm{M}}^{\mathrm{UL}} = \frac{P_{t,v}^{\mathrm{UL}}|h_{\mathrm{M}}|r_{\mathrm{M}}^{-\alpha}}{I_{\phi_{\mathrm{M}},A_{\mathrm{M}}^o}^{\mathrm{UL}} + I_{\phi_{\mathrm{S}},A_{\mathrm{M}}^c}^{\mathrm{DL}} + I_{\phi_{\mathrm{D}},A_{\mathrm{M}}^c}^{\mathrm{DL}}}. \tag{4}$$

Eq. (4) can be further expanded as

$$\mathrm{SIR}_{\mathrm{M}}^{\mathrm{UL}} = \frac{P_{t,v}^{\mathrm{UL}}|h_{\mathrm{M}}|r_{\mathrm{M}}^{-\alpha}}{\sum\limits_{l\in\phi_{\mathrm{M}}} P_{t,l}^{\mathrm{UL}}|h_l|r_l^{-\alpha} + \sum\limits_{k\in\phi_{\mathrm{S}}} P_{t,k}^{\mathrm{DL}}|h_k|r_k^{-\alpha} + \sum\limits_{j\in\phi_{\mathrm{D}}} P_{t,j}^{\mathrm{DL}}|h_j|r_j^{-\alpha}}. \tag{5}$$

Here, $P_{t,l}^{\mathrm{UL}}$ denotes the UL transmit power of MBS associated v, $P_{t,k}^{\mathrm{DL}}$ indicates the SBS transmit power in DL, and $P_{t,j}^{\mathrm{DL}}$ is the drones transmit power in DL. Now, by substituting (4) into (3), we obtain $P_{A_{\mathrm{M}}^o}^{\mathrm{UL}''}(\gamma_{\mathrm{M}})$ as

$$\begin{aligned}
&P_{A_{\mathrm{M}}^o}^{\mathrm{UL}''}(\gamma_{\mathrm{M}}) \\
&= P\left(\frac{P_{t,v}^{\mathrm{UL}}|h_{\mathrm{M}}|r_{\mathrm{M}}^{-\alpha}}{I_{\phi_{\mathrm{M}},A_{\mathrm{M}}^o}^{\mathrm{UL}} + I_{\phi_{\mathrm{S}},A_{\mathrm{M}}^c}^{\mathrm{DL}} + I_{\phi_{\mathrm{D}},A_{\mathrm{M}}^c}^{\mathrm{DL}}} > \gamma_{\mathrm{M}}\right) \\
&= \mathbb{E}_{r_{\mathrm{M}},I_{\phi_{\mathrm{M}},A_{\mathrm{M}}^o}^{\mathrm{UL}},I_{\phi_{\mathrm{S}},A_{\mathrm{M}}^c}^{\mathrm{DL}},I_{\phi_{\mathrm{D}},A_{\mathrm{M}}^c}^{\mathrm{DL}}} \\
&\quad\times\left[\exp\left(-\frac{r_{\mathrm{M}}^{\alpha}\gamma_{\mathrm{M}}}{P_{t,v}^{\mathrm{UL}}}\left(I_{\phi_{\mathrm{M}},A_{\mathrm{M}}^o}^{\mathrm{UL}} + I_{\phi_{\mathrm{S}},A_{\mathrm{M}}^c}^{\mathrm{DL}} + I_{\phi_{\mathrm{D}},A_{\mathrm{M}}^c}^{\mathrm{DL}}\right)\right)\right] \\
&= \mathbb{E}_{r_{\mathrm{M}}}\left[\mathcal{L}_{I_{\phi_{\mathrm{M}},A_{\mathrm{M}}^o}^{\mathrm{UL}}}(s)\times\mathcal{L}_{I_{\phi_{\mathrm{S}},A_{\mathrm{M}}^c}^{\mathrm{DL}}}(s)\times\mathcal{L}_{I_{\phi_{\mathrm{D}},A_{\mathrm{M}}^c}^{\mathrm{DL}}}(s)\right]\Big|_{s=\frac{r_{\mathrm{M}}^{\alpha}\gamma_{\mathrm{M}}}{P_{t,v}^{\mathrm{UL}}}},
\end{aligned} \tag{6}$$

where $\mathcal{L}(\cdot)$ denotes the LT.

The LT of the interference from MBS-tier in UL, i.e., $\mathcal{L}_{I_{\phi_{\mathrm{M}},A_{\mathrm{M}}^o}^{\mathrm{UL}}}(s)$, is obtained as

$$\begin{aligned}
&\mathcal{L}_{I_{\phi_{\mathrm{M}},A_{\mathrm{M}}^o}^{\mathrm{UL}}}(s) \\
&= \exp\Bigg(\frac{\rho_{\mathrm{M}}\pi\gamma_{\mathrm{M}}d_2^{(2-\alpha)}r_{\mathrm{M}}^{\alpha}}{\alpha/2-1}\,{}_2F_1 \\
&\quad\left(1, 1-\frac{2}{\alpha}, 2-\frac{2}{\alpha}, -\gamma_{\mathrm{M}}\left(\frac{r_{\mathrm{M}}}{d_2}\right)^{\alpha}\right) \\
&\quad-\frac{\rho_{\mathrm{M}}\pi\gamma_{\mathrm{M}}d_1^{(2-\alpha)}r_{\mathrm{M}}^{\alpha}}{\alpha/2-1}\,{}_2F_1 \\
&\quad\times\left(1, 1-\frac{2}{\alpha}, 2-\frac{2}{\alpha}, -\gamma_{\mathrm{M}}\left(\frac{r_{\mathrm{M}}}{d_1}\right)^{\alpha}\right)\Bigg).
\end{aligned} \tag{7}$$

Proof: The proof of (7) is given in Appendix A.

We obtain the LT of the interference from SBSs in DL, i.e., $\mathcal{L}_{I^{\mathrm{DL}}_{\phi_{\mathrm{S}},A^o_{\mathrm{M}}}}(s)$, in a way similar to (7), and given as

$$\begin{aligned}\mathcal{L}_{I^{\mathrm{DL}}_{\phi_{\mathrm{S}},A^o_{\mathrm{M}}}}(s) &= \exp\Bigg(\frac{\rho_{\mathrm{S}}\pi\zeta_1\gamma_{\mathrm{M}}x_2^{(2-\alpha)}r_{\mathrm{M}}^{\alpha}}{\alpha/2-1}\,{}_2F_1\\ &\left(1,1-\frac{2}{\alpha},2-\frac{2}{\alpha},-\zeta_1\gamma_{\mathrm{M}}\left(\frac{r_{\mathrm{M}}}{x_2}\right)^{\alpha}\right)\\ &-\frac{\rho_{\mathrm{S}}\pi\zeta_1\gamma_{\mathrm{M}}x_1^{(2-\alpha)}r_{\mathrm{M}}^{\alpha}}{\alpha/2-1}\,{}_2F_1\\ &\times\left(1,1-\frac{2}{\alpha},2-\frac{2}{\alpha},-\zeta_1\gamma_{\mathrm{M}}\left(\frac{r_{\mathrm{M}}}{x_1}\right)^{\alpha}\right)\Bigg). \qquad (8)\end{aligned}$$

Here, ζ_1 is the ratio of $P^{\mathrm{DL}}_{t,\mathrm{S}}$ and $P^{\mathrm{UL}}_{t,\nu}$, where $P^{\mathrm{DL}}_{t,\mathrm{S}}$ is the SBS DL transmit power.

From (8), the LT of the interference from SBSs in UL, i.e., $\mathcal{L}_{I^{\mathrm{UL}}_{\phi_{\mathrm{S}},A^o_{\mathrm{M}}}}(s)$, is obtained as

$$\mathcal{L}_{I^{\mathrm{UL}}_{\phi_{\mathrm{S}},A^o_{\mathrm{M}}}}(s) = \left(\mathcal{L}_{I^{\mathrm{DL}}_{\phi_{\mathrm{S}},A^o_{\mathrm{M}}}}\right)\backslash\zeta_1, \qquad (9)$$

where $(\cdot)\backslash\zeta_1$ denotes the exclusion of ζ_1 from (8).

The LT of DI due to EDU, i.e., $\mathcal{L}_{I^{\mathrm{DL}}_{\phi_{\mathrm{D}},A^c_{\mathrm{M}}}}(s)$, can be given as

$$\begin{aligned}\mathcal{L}_{I^{\mathrm{DL}}_{\phi_{\mathrm{D}},A^c_{\mathrm{M}}}}(s) &= \exp\Bigg(\frac{\rho_{\mathrm{D}}\pi\zeta_2\gamma_{\mathrm{M}}d_1^{(2-\alpha)}r_{\mathrm{M}}^{\alpha}}{\alpha/2-1}\,{}_2F_1\\ &\left(1,1-\frac{2}{\alpha},2-\frac{2}{\alpha},-\zeta_2\gamma_{\mathrm{M}}\left(\frac{r_{\mathrm{M}}}{d_1}\right)^{\alpha}\right)\\ &-\frac{\rho_{\mathrm{D}}\pi\zeta_2\gamma_{\mathrm{M}}y^{(2-\alpha)}r_{\mathrm{M}}^{\alpha}}{\alpha/2-1}\,{}_2F_1\\ &\times\left(1,1-\frac{2}{\alpha},2-\frac{2}{\alpha},-\zeta_2\gamma_{\mathrm{M}}\left(\frac{r_{\mathrm{M}}}{y}\right)^{\alpha}\right)\Bigg). \qquad (10)\end{aligned}$$

In (10), ζ_2 is the ratio of $P^{\mathrm{DL}}_{t,\mathrm{D}}$ and $P^{\mathrm{UL}}_{t,\nu}$, where $P^{\mathrm{DL}}_{t,\mathrm{D}}$ is the transmit power of drones in A^c_{M}. y and d_1 define the interfering drones area, s.t., $y < d_1$.

Proof: See Appendix B for the proof of (10).

Given that $\nu \in A^o_{\mathrm{M}}$, i.e., $\nu_{A^o_{\mathrm{M}}}$, and associated with MBS at a distance r_{M}, has the PDF of distances given as [38]

$$f_{r_{\mathrm{M}}|\nu_{A^o_{\mathrm{M}}}}(r_{\mathrm{M}}) = \frac{2\pi\rho_{\mathrm{M}}r_{\mathrm{M}}\exp\left(-\rho_{\mathrm{M}}\pi r_{\mathrm{M}}^2\right)}{\exp\left(-\rho_{\mathrm{M}}\pi d_1^2\right)}. \qquad (11)$$

Similarly, assuming that $\nu \in A^o_{\mathrm{M}}$, i.e., $\nu_{A^o_{\mathrm{S}}}$, and associated with SBS at a distance r_{S}, has the PDF of distances given as

$$f_{r_{\mathrm{S}}|\nu_{A^o_{\mathrm{S}}}}(r_{\mathrm{S}}) = \frac{2\pi\rho_{\mathrm{S}}r_{\mathrm{S}}\exp\left(-\rho_{\mathrm{S}}\pi r_{\mathrm{S}}^2\right)}{\exp\left(-\rho_{\mathrm{M}}\pi d_1^2\right)}. \qquad (12)$$

The UL coverage probability expression, i.e., $P^{\mathrm{UL}''}_{A^o_{\mathrm{M}}}(\gamma_{\mathrm{M}})$, for ν associated with MBS in A^o_{M} while considering EDU, RFA, and CA can be written as [39]

$$P^{\mathrm{UL}''}_{A^o_{\mathrm{M}}}(\gamma_{\mathrm{M}}) = \int_{d_1}^{d_2}\mathcal{L}_{I^{\mathrm{UL}}_{\phi_{\mathrm{M}},A^o_{\mathrm{M}}}}(s)\times\mathcal{L}_{I^{\mathrm{DL}}_{\phi_{\mathrm{S}},A^c_{\mathrm{M}}}}(s)\times\mathcal{L}_{I^{\mathrm{DL}}_{\phi_{\mathrm{D}},A^c_{\mathrm{M}}}}(s) \times f_{r_{\mathrm{M},\nu}|\nu_{A^o_{\mathrm{M}}}}\left(r_{\mathrm{M},\nu}\right)dr_{\mathrm{M},\nu}. \qquad (13)$$

By substituting (7), (8), (10), and (11) into (13), the expression for UL coverage probability, given that ν is associated with MBS in A^o_{M}, can be written as (14), shown at the bottom of the next page. In (14), $\mathcal{J}(\cdot)$ indicates the Gauss-hypergeometric function.

B. UL COVERAGE PROBABILITY WITH DeCA

The UL coverage probability expression, i.e., $P^{\mathrm{UL}'}_{A^o_{\mathrm{M}}}(\gamma_{\mathrm{S}})$, assuming EDU, RFA and DeCA, can be written as [29], [40]

$$P^{\mathrm{UL}'}_{A^o_{\mathrm{M}}}(\gamma_{\mathrm{S}}) = \int_{d_1}^{d_2}\left[\mathcal{L}_{I^{\mathrm{UL}}_{\phi_{\mathrm{S}},A^c_{\mathrm{M}}}}(s)\times\mathcal{L}_{I^{\mathrm{DL}}_{\phi_{\mathrm{S}},A^o_{\mathrm{M}}}}(s)\times\mathcal{L}_{I^{\mathrm{DL}}_{\phi_{\mathrm{D}},A^c_{\mathrm{M}}}}(s)\right] \times f_{r_{\mathrm{S}}|U_{A^o_{\mathrm{M}}}}(r_{\mathrm{S}})\,dr_{\mathrm{S}}. \qquad (16)$$

By substituting (8), (9), (10) and (12) into (16), $P^{\mathrm{UL}'}_{A^o_{\mathrm{M}}}(\gamma_{\mathrm{S}})$ can be expressed as (15), shown at the bottom of the next page.

IV. RESULTS AND DISCUSSION

This section presents simulation and numerical results for the UL coverage probability given that $\nu \in A^o_{\mathrm{M}}$, while considering EDU and RFA for (i) CA, and (ii) DeCA. A is taken as $\pi(1000\mathrm{m})^2$, s.t., $A = A^c_{\mathrm{M}}\mathrm{U}A^o_{\mathrm{M}}$. Moreover, transmit powers of MBS, SBS, UE, and drone are configured as 40 dBm,

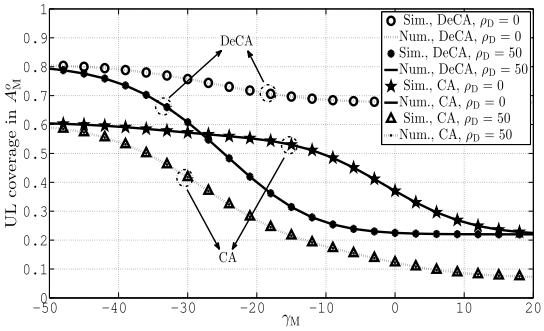

FIGURE 3. UL coverage in A^o_{M} with CA and DeCA.

TABLE 2. Simulation parameters.

Parameter	Configuration
MBS, SBS, and drone distributions	IHPPP
Code iterations	5000
ρ_{S}	$15/\pi(1000\mathrm{m})^2$
ρ_{M}	$3/\pi(1000\mathrm{m})^2$
ρ_{D}	$50/\pi(100\mathrm{m})^2$
$P^{\mathrm{UL}}_{t,\mathrm{M}}$, $P^{\mathrm{DL}}_{t,\mathrm{S}}$, $P^{\mathrm{UL}}_{t,\nu}$, $P^{\mathrm{DL}}_{t,\mathrm{D}}$	40 dBm, 30 dBm, 20 dBm and 20 dBm, respectively
$\alpha_m = \alpha_s = \alpha$	3

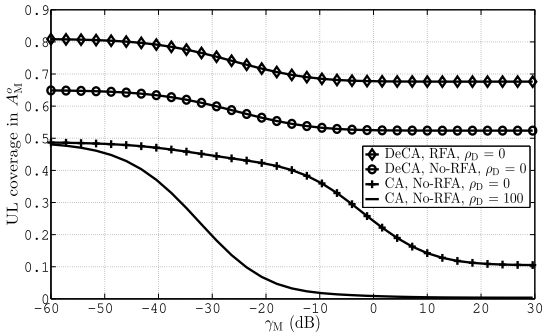

FIGURE 4. UL coverage in A_M^o with and without RFA.

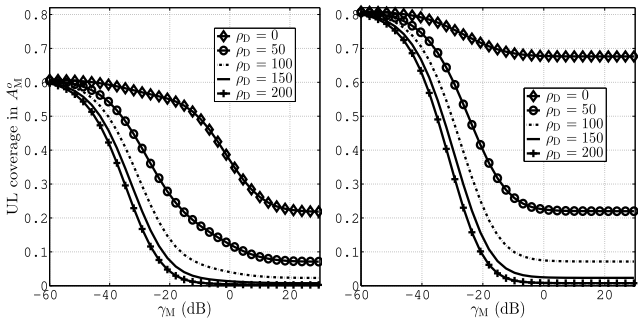

(a) CA with RFA (b) DeCA with RFA

FIGURE 5. UL coverage in A_M^o against γ_M and ρ_D.

30 dBm, 20 dBm, and 20 dBm, respectively. Mathematica 11 and MATLAB 2017B have been used to derive and evaluate the coverage probability expressions.

In Figs. 3 and 4, we measure the UL coverage against the predefined threshold, γ_M, and different values of ρ_D while assuming different network scenarios, such as with and without CA, with and without DeCA, and with and without RFA. In Fig. 3, we compute numerical and simulation results for the UL coverage probabilities taking CA and DeCA into account. This figure validates (14) and (15) and points toward improved UL coverage with DeCA as compared with CA. Moreover, the plots in Fig. 3 indicate that increase in the the values of ρ_D reduces the UL coverage.

The plots in Fig. 4 indicate significant coverage improvement by using RFA as compared with the conventional methods. This is due to the fact that by using RFA, the interference received by ν from drones located in A_M^c is neglected. Moreover, the results demonstrate that DeCA outperforms CA due to users' association with the closest BSs. Furthermore, the results depict that the UL coverage degrades significantly when $\rho_D = 100$. Furthermore, the plots in Fig. 4 indicate 16% UL coverage improvement as observed at $\gamma_M = -10$ dB by DeCA with RFA, as compared to CA with RFA.

Figs. 5(a) and 5(b) measure the UL coverage probabilities against ρ_D while employing CA and DeCA. Both these figures indicate that the UL coverage considerably degrades with an increase in ρ_D. This is due to the fact that an increase in the values of ρ_D leads to severe DI. However, Fig. 5(b) indicates improved UL coverage as compared with Fig. 5(a) due to effective interference mitigation by using both DeCA and RFA. Moreover, Figs. 5(a) and 5(b) indicate that, at $\gamma_M = -10$ dB and $\rho_D = 50$, DeCA with RFA leads to 8% UL coverage improvement as opposed to CA with RFA.

In Figs. 6(a) and 6(b), we present the UL coverage probabilities against different values of $P_{t,D}^{DL}$ and ρ_D taking CA and DeCA into account, respectively. In both the figures, the value of $P_{t,D}^{DL}$ ranges from 20 dB to 100 dB while $\rho_D = 0, 10, 20, 30, 40$, and 50. The figures depict that an increase in the value of $P_{t,D}^{DL}$ and ρ_D leads to reduced UL coverage because of higher DI. This is due to the fact that an increase in the values of $P_{t,D}^{DL}$ and ρ_D leads to significant DI. Moreover, in Fig. 6(b),

$$P_{A_M^o}^{UL''}(\gamma_M) = \frac{2\pi\rho_M}{\exp\left(-\rho_M\pi d_1^2\right)} \int_{d_1}^{d_2} \exp\left(\frac{\pi\gamma_M r_M^\alpha}{\alpha/2-1}\left[\rho_M d_2^{(2-\alpha)}\mathcal{J}\left(\alpha, -\gamma_M\left(\frac{r_M}{d_2}\right)^\alpha\right) - \rho_M d_1{}^{(2-\alpha)}\mathcal{J}\left(\alpha, -\gamma_M\left(\frac{r_M}{d_1}\right)^\alpha\right)\right.\right.$$
$$+\rho_S\zeta_1\, d_1^{(2-\alpha)}\mathcal{J}\left(\alpha, -\gamma_M\zeta_1\left(\frac{r_M}{d_1}\right)^\alpha\right) - \rho_S\zeta_1\, y^{(2-\alpha)}\mathcal{J}\left(\alpha, -\gamma_M\zeta_1\left(\frac{r_M}{y}\right)^\alpha\right) + \rho_D\zeta_2\, d_2^{(2-\alpha)}\mathcal{J}\left(\alpha, -\gamma_M\zeta_2\left(\frac{r_M}{d_2}\right)^\alpha\right)$$
$$\left.\left.-\rho_D\zeta_2\, y^{(2-\alpha)}\mathcal{J}\left(\alpha, -\gamma_M\zeta_2\left(\frac{r_M}{y}\right)^\alpha\right)\right] - \rho_M\pi r_M^2\right) r_M dr_M. \quad (14)$$

$$P_{A_M^o}^{UL'}(\gamma_S) = \frac{2\pi\rho_S}{\exp\left(-\rho_M\pi d_1^2\right)} \int_{d_1}^{d_2} \exp\left(\frac{\pi\rho_S r_S^\alpha\gamma_S}{\alpha/2-1}\left[x_2^{(2-\alpha)}\zeta_1\mathcal{J}\left(\alpha, -\zeta_1\gamma_S\left(\frac{r_S}{x_2}\right)^\alpha\right) - x_1^{(2-\alpha)}\zeta_1\mathcal{J}\left(\alpha, -\zeta_1\gamma_S\left(\frac{r_S}{x_1}\right)^\alpha\right)\right.\right.$$
$$+x_2^{(2-\alpha)}\mathcal{J}\left(\alpha, -\gamma_S\left(\frac{r_S}{x_2}\right)^\alpha\right) - x_1^{(2-\alpha)}\mathcal{J}\left(\alpha, -\gamma_S\left(\frac{r_S}{x_1}\right)^\alpha\right) + \rho_D\zeta_2\, d_2^{(2-\alpha)}\mathcal{J}\left(\alpha, -\gamma_M\zeta_2\left(\frac{r_M}{d_2}\right)^\alpha\right)$$
$$\left.\left.-\rho_D\zeta_2\, y^{(2-\alpha)}\mathcal{J}\left(\alpha, -\gamma_M\zeta_2\left(\frac{r_M}{y}\right)^\alpha\right)\right] - \rho_S\pi r_S^2\right) r_S dr_S. \quad (15)$$

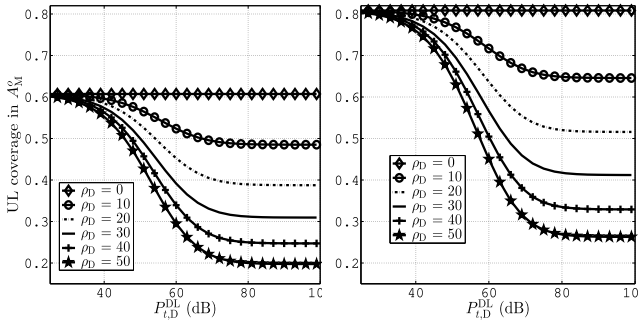

(a) CA with RFA (b) DeCA with RFA

FIGURE 6. UL coverage in A^o_M against $P^{DL}_{t,D}$ and ρ_D.

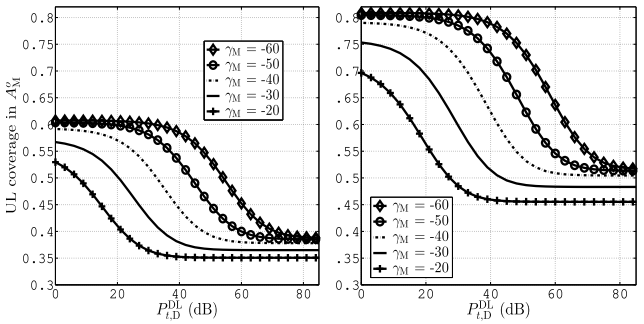

(a) CA with RFA (b) DeCA with RFA

FIGURE 7. UL coverage in A^o_M against $P^{DL}_{t,D}$ and γ_M.

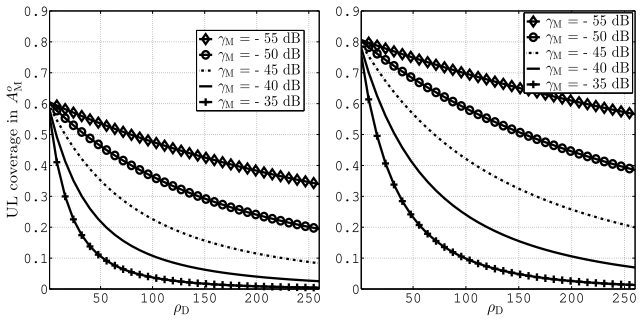

(a) CA with RFA (b) DeCA with RFA

FIGURE 8. UL coverage in A^o_M for CA, DeCA, and different configurations of γ_M and ρ_D.

we show significant improvement in the UL coverage due to DeCA and RFA as compared to CA and RFA in Fig. 6(a).

Figs. 7(a) and 7(b) present the UL coverage probabilities against $P^{DL}_{t,D}$ and γ_M while employing CA and DeCA. The plots in the figures show that raising values of $P^{DL}_{t,D}$ causes reduced UL coverage as a result of higher DI. Moreover, the plots in the figure show that lower values of γ_M cause higher UL coverage due to improved users association. Furthermore, the results indicate that RFA with DeCA provides improved UL coverage.

Next, in Figs. 8(a) and 8(b), we compute the UL coverage probability for different values of ρ_D and γ_M. The figures indicate that raising the values of γ_M causes lower UL coverage due to lower user associations. Moreover, an increase in the values of ρ_D causes reduced UL coverage because of higher DI. Furthermore, the figures indicate that DeCA in conjunction RFA overpass all other scenarios due to efficient ICI and DI management.

V. CONCLUSION

In 5G networks, SBS densification in the MBS coverage area give rise to improved spectral efficiency and capacity, however, this causes significant ICI. Moreover, 5G assisted EDU imposes considerable DI on the network. To mitigate both DI and ICI, we use RFA along with DeCA. The results depict that higher values of $P^{DL}_{t,D}$ and ρ_D cause lower UL coverage for ν which is located in A^o_M. Moreover, the results show that RFA and DeCA lead to significant UL coverage improvement and, thus, outperform all other techniques. This work can be further extended by incorporating fractional power control in the proposed setup.

APPENDIX A
PROOF OF THE LT OF (7)

Proof of (7): The LT of the UL interference from MBS-tier in A^o_M, i.e., $\mathcal{L}_{I^{UL}_{\phi_M,A^o_M}}(s)$, is obtained as

$$
\begin{aligned}
&\mathcal{L}_{I^{UL}_{\phi_M,A^o_M}}(s)\\
&\overset{(a)}{=} \mathbb{E}_{I^{UL}_{\phi_M,A^o_M}}\left[\exp\left(-I^{UL}_{\phi_M,A^o_M}s\right)\right]\Big|_{s=\frac{r_M^{\alpha}\gamma_M}{P^{UL}_{t,\nu}}}\\
&\overset{(b)}{=} \mathbb{E}_{I^{UL}_{\phi_M,A^o_M},|h_l|}\left[\exp\left(-s\sum_{l\in\phi_M}P^{UL}_{t,\nu}|h_l|r_l^{-\alpha}\right)\right]\\
&\overset{(c)}{=} \mathbb{E}_{I^{UL}_{\phi_M,A^o_M},|h_l|}\left[\prod_{l\in\phi_M}\exp\left(-|h_l|\gamma_M r_M^{\alpha}r_l^{-\alpha}\right)\right]\\
&\overset{(d)}{=} \mathbb{E}_{I^{UL}_{\phi_M,A^o_M}}\left[\prod_{l\in\phi_M}\mathbb{E}_{|h_l|}\exp\left(-|h_l|\gamma_M r_M^{\alpha}r_l^{-\alpha}\right)\right]\\
&\overset{(e)}{=} \mathbb{E}_{I^{UL}_{\phi_M,A^o_M}}\left[\prod_{l\in\phi_M}\frac{1}{1+\gamma_M\left((r_M)^{-1}r_l\right)^{-\alpha}}\right]\\
&\overset{(f)}{=} \exp\left(-2\pi\rho_M\int_{d_1}^{d_2}\frac{r_l dr_l}{1+\left(\frac{r_l}{\gamma_M^{1/\alpha}r_M}\right)^{\alpha}}\right)\\
&\overset{(g)}{=} \exp\left(-\pi\rho_M\gamma_M^{2/\alpha}r_M^2\int_{\left(\frac{d_1}{\gamma_M^{1/\alpha}r_M}\right)^2}^{\left(\frac{d_2}{\gamma_M^{1/\alpha}r_M}\right)^2}\frac{du}{1+(u)^{\alpha/2}}\right),
\end{aligned}
\tag{17}
$$

where equality (a) is achieved by following LT definition [20], equality (b) is achieved by replacing $I^{\mathrm{UL}}_{\phi_{\mathrm{M}},A^o_{\mathrm{M}}} = \sum_{l\in\phi_{\mathrm{M}}} P^{\mathrm{UL}}_{t,l}|h_l|r_l^{-\alpha}$ into equality (a), equality (c) is achieved by replacing $s = \left(r^{\alpha}_{\mathrm{M}}\beta_{\mathrm{M}}\right)/\left(P^{\mathrm{UL}}_{t,\nu}\right)$ into equality (b), equality (e) is achieved by evaluating the LT of equality (d) in terms of h_j, equality (f) is achieved from probability generating functional (PGFL) of IHPPP [39], and equality (g) is achieved by replacing $u = \left(r_l/(\gamma_{\mathrm{M}})^{1/\alpha}r_{\mathrm{M}}\right)^2$ into equality (f). Lastly, employing Gauss-hypergeometric function [20] yields (7). ■

APPENDIX B
PROOF OF THE LT OF (10)

Proof of (10): The LT of DI received from EDU, i.e., $\mathcal{L}_{I^{\mathrm{DL}}_{\phi_{\mathrm{D}},A^c_{\mathrm{M}}}}(s)$, can be shown as

$$\begin{aligned}
&\mathcal{L}_{I^{\mathrm{DL}}_{\phi_{\mathrm{D}},A^c_{\mathrm{M}}}}(s)\\
&\overset{(h)}{=} \mathbb{E}_{I^{\mathrm{DL}}_{\phi_{\mathrm{D}},A^c_{\mathrm{M}}}}\left[\exp\left(-I^{\mathrm{DL}}_{\phi_{\mathrm{D}},A^c_{\mathrm{M}}}s\right)\right]\Big|_{s=\frac{r^{\alpha}_{\mathrm{M}}\gamma_{\mathrm{M}}}{P^{\mathrm{UL}}_{t,\nu}}}\\
&\overset{(i)}{=} \mathbb{E}_{I^{\mathrm{DL}}_{\phi_{\mathrm{D}},A^c_{\mathrm{M}}},|h_j|}\left[\exp\left(-s\sum_{j\in\phi_{\mathrm{D}}}P^{\mathrm{DL}}_{t,j}|h_j|r_j^{-\alpha}\right)\right]\\
&\overset{(j)}{=} \mathbb{E}_{I^{\mathrm{DL}}_{\phi_{\mathrm{D}},A^c_{\mathrm{M}}},|h_j|}\left[\prod_{j\in\phi_{\mathrm{D}}}\exp\left(-|h_j|\zeta_2\gamma_{\mathrm{M}}r^{\alpha}_{\mathrm{M}}r_j^{-\alpha}\right)\right]\\
&\overset{(k)}{=} \mathbb{E}_{I^{\mathrm{DL}}_{\phi_{\mathrm{D}},A^c_{\mathrm{M}}}}\left[\prod_{j\in\phi_{\mathrm{D}}}\mathbb{E}_{|h_j|}\exp\left(-|h_j|\zeta_2\gamma_{\mathrm{M}}r^{\alpha}_{\mathrm{M}}r_j^{-\alpha}\right)\right]\\
&\overset{(l)}{=} \mathbb{E}_{I^{\mathrm{DL}}_{\phi_{\mathrm{D}},A^c_{\mathrm{M}}}}\left[\prod_{j\in\phi_{\mathrm{D}}}\frac{1}{1+\zeta_2\gamma_{\mathrm{M}}\left(r_j(r_{\mathrm{M}})^{-1}\right)^{-\alpha}}\right]\\
&\overset{(m)}{=} \exp\left(-2\pi\rho_{\mathrm{D}}\int_{y}^{d_1}\frac{r_j dr_j}{1+\left(\frac{r_j}{(\zeta_2\gamma_{\mathrm{M}})^{1/\alpha}r_{\mathrm{M}}}\right)^{\alpha}}\right)\\
&\overset{(n)}{=} \exp\left(-\pi\rho_{\mathrm{D}}(\zeta_2\gamma_{\mathrm{M}})^{2/\alpha}r^2_{\mathrm{M}}\int_{\left(\frac{y}{(\zeta_2\gamma_{\mathrm{M}})^{1/\alpha}r_{\mathrm{M}}}\right)^2}^{\left(\frac{d_1}{(\zeta_2\gamma_{\mathrm{M}})^{1/\alpha}r_{\mathrm{M}}}\right)^2}\frac{du}{1+(u)^{\alpha/2}}\right).
\end{aligned} \tag{18}$$

Here, equality (h) is achieved from the LT definition [20], equality (i) is achieved by replacing $I^{\mathrm{DL}}_{\phi_{\mathrm{D}},A^c_{\mathrm{M}}} = \sum_{j\in\phi_{\mathrm{D}}}P^{\mathrm{DL}}_{t,j}|h_j|r_j^{-\alpha}$ into equality (h), equality (j) is achieved by replacing $s = \left(r^{\alpha}_{\mathrm{M}}\beta_{\mathrm{M}}\right)/\left(P^{\mathrm{UL}}_{t,\nu}\right)$ into equality (i), equality (l) is achieved by evaluating the LT of equality (k) with respect to h_j, equality (m) is achieved by using PGFL of IHPPP, and equality (n) is achieved by replacing $u = \left(r_j/(\zeta_2\gamma_{\mathrm{M}})^{1/\alpha}r_{\mathrm{M}}\right)^2$ into equality (m). Finally, by employing Gauss-hypergeometric function to equality (n), we obtain the expression given in (10) ■

REFERENCES

[1] D. B. Da Costa, T. Q. Duong, M. A. Imran, H. Q. Ngo, N. Yang, and O. A. Dobre, "Modeling, analysis, and design of 5G ultra-dense networks," *IEEE Access*, vol. 7, pp. 18894–18898, 2019.
[2] J. G. Andrews, S. Buzzi, W. Choi, S. V. Hanly, A. Lozano, A. C. K. Soong, and J. C. Zhang, "What will 5G be?" *IEEE J. Sel. Areas Commun.*, vol. 32, no. 6, pp. 1065–1082, Jun. 2014.
[3] M. S. Akhtar, Z. H. Abbas, F. Muhammad, and G. Abbas, "Analysis of decoupled association in HetNets using soft frequency reuse scheme," *AEU-Int. J. Electron. Commun.*, vol. 113, Jan. 2020, Art. no. 152961.
[4] M. S. Haroon, F. Muhammad, Z. H. Abbas, G. Abbas, N. Ahmed, and S. Kim, "Proactive uplink interference management for nonuniform heterogeneous cellular networks," *IEEE Access*, vol. 8, pp. 55501–55512, 2020.
[5] P. Chandhar and E. G. Larsson, "Massive MIMO for connectivity with drones: Case studies and future directions," *IEEE Access*, vol. 7, pp. 94676–94691, 2019.
[6] L. Zhang, H. Zhao, S. Hou, Z. Zhao, H. Xu, X. Wu, Q. Wu, and R. Zhang, "A survey on 5G millimeter wave communications for UAV-assisted wireless networks," *IEEE Access*, vol. 7, pp. 117460–117504, 2019.
[7] Michael Thomsen For Dailymail.com. (Oct. 2019). *UPS Receives Government Approval for Drone Delivery-Beating Out Amazon and Alphabet*. [Online]. Available: https://www.dailymail.co.uk/sciencetech/article-7530063.html
[8] H. Ullah, N. G. Nair, A. Moore, C. Nugent, P. Muschamp, and M. Cuevas, "5G communication: An overview of vehicle-to-everything, drones, and healthcare use-cases," *IEEE Access*, vol. 7, pp. 37251–37268, 2019.
[9] A. Simonsson and T. Andersson, "LTE uplink CoMP trial in a HetNet deployment," in *Proc. IEEE Veh. Technol. Conf. (VTC Fall)*, Sep. 2012, pp. 1–5.
[10] O. Chabbouh, S. B. Rejeb, Z. Choukair, and N. Agoulmine, "Offloading decision algorithm for 5G/HetNets cloud RAN," in *Proc. 24th Int. Conf. Softw., Telecommun. Comput. Netw. (SoftCOM)*, Sep. 2016, pp. 1–5.
[11] M. S. Haroon, Z. H. Abbas, F. Muhammad, and G. Abbas, "Coverage analysis of cell-edge users in heterogeneous wireless networks using Stienen's model and RFA scheme," *Int. J. Commun. Syst.*, p. e4147, Sep. 2019, doi: 10.1002/dac.4147.
[12] M. N. Sial and J. Ahmed, "A realistic uplink-downlink coupled and decoupled user association technique for K-tier 5G HetNets," *Arabian J. Sci. Eng.*, vol. 44, no. 3, pp. 2185–2204, Mar. 2019.
[13] M. S. Haroon, Z. H. Abbas, G. Abbas, and F. Muhammad, "Coverage analysis of ultra-dense heterogeneous cellular networks with interference management," *Wireless Netw.*, vol. 26, no. 3, pp. 2013–2025, Feb. 2019, doi: 10.1007/s11276-019-01965-0.
[14] A. Ullah, Z. H. Abbas, G. Abbas, and F. Muhammad, "Analysis of outage probability and rate coverage in heterogeneous cellular network with joint uniform and clustered users," in *Proc. 22nd Int. Multitopic Conf. (INMIC)*, Nov. 2019, pp. 1–7.
[15] X. Jia, Q. Fan, W. Xu, and L. Yang, "Cross-tier dual-connectivity designs of three-tier hetnets with decoupled uplink/downlink and global coverage performance evaluation," *IEEE Access*, vol. 7, pp. 16816–16836, 2019.
[16] M. S. Haroon, Z. H. Abbas, G. Abbas, and F. Muhammad, "Analysis of interference mitigation in heterogeneous cellular networks using soft frequency reuse and load balancing," in *Proc. 28th Int. Telecommun. Netw. Appl. Conf. (ITNAC)*, Nov. 2018, pp. 1–6.
[17] M. Fereydooni, M. Sabaei, M. Dehghan, G. B. Eslamlou, and M. Rupp, "Analytical evaluation of heterogeneous cellular networks under flexible user association and frequency reuse," *Comput. Commun.*, vol. 116, pp. 147–158, Jan. 2018.
[18] S. Hashima, O. Muta, M. Alghonimey, H. Shalaby, H. Frukawa, S. Elnoubi, and I. Mahmoud, "Area spectral efficiency performance comparison of downlink fractional frequency reuse schemes for MIMO heterogeneous networks," in *Proc. Int. Conf. Inf. Sci., Electron. Electr. Eng.*, vol. 2, Apr. 2014, pp. 1005–1010.

[19] M. M. Pervez, Z. H. Abbas, F. Muhammad, and L. Jiao, "Location-based coverage and capacity analysis of a two tier HetNet," *IET Commun.*, vol. 11, no. 7, pp. 1067–1073, May 2017.
[20] M. S. Haroon, Z. H. Abbas, F. Muhammad, and G. Abbas, "Analysis of coverage-oriented small base station deployment in heterogeneous cellular networks," *Phys. Commun.*, vol. 38, Feb. 2020, Art. no. 100908.
[21] Z. H. Abbas, F. Muhammad, and L. Jiao, "Analysis of load balancing and interference management in heterogeneous cellular networks," *IEEE Access*, vol. 5, pp. 14690–14705, 2017.
[22] Z. H. Abbas, M. S. Haroon, G. Abbas, and F. Muhammad, "SIR analysis for non-uniform HetNets with joint decoupled association and interference management," *Comput. Commun.*, vol. 155, pp. 48–57, Apr. 2020.
[23] A. Orsino, A. Ometov, G. Fodor, D. Moltchanov, L. Militano, S. Andreev, O. N. C. Yilmaz, T. Tirronen, J. Torsner, G. Araniti, A. Iera, M. Dohler, and Y. Koucheryavy, "Effects of heterogeneous mobility on D2D- and drone-assisted mission-critical MTC in 5G," *IEEE Commun. Mag.*, vol. 55, no. 2, pp. 79–87, Feb. 2017.
[24] Z. Kaleem and M. H. Rehmani, "Amateur drone monitoring: State-of-the-art architectures, key enabling technologies, and future research directions," *IEEE Wireless Commun.*, vol. 25, no. 2, pp. 150–159, Apr. 2018.
[25] S. A. R. Naqvi, S. A. Hassan, H. Pervaiz, and Q. Ni, "Drone-aided communication as a key enabler for 5G and resilient public safety networks," *IEEE Commun. Mag.*, vol. 56, no. 1, pp. 36–42, Jan. 2018.
[26] A. Fotouhi, M. Ding, and M. Hassan, "DroneCells: Improving 5G spectral efficiency using drone-mounted flying base stations," 2017, *arXiv:1707.02041*. [Online]. Available: http://arxiv.org/abs/1707.02041
[27] S. Sekander, H. Tabassum, and E. Hossain, "Multi-tier drone architecture for 5G/B5G cellular networks: Challenges, trends, and prospects," *IEEE Commun. Mag.*, vol. 56, no. 3, pp. 96–103, Mar. 2018.
[28] T. Hou, Y. Liu, Z. Song, X. Sun, and Y. Chen, "Multiple antenna aided NOMA in UAV networks: A stochastic geometry approach," *IEEE Trans. Commun.*, vol. 67, no. 2, pp. 1031–1044, Feb. 2019.
[29] F. Muhammad, Z. H. Abbas, G. Abbas, and L. Jiao, "Decoupled downlink-uplink coverage analysis with interference management for enriched heterogeneous cellular networks," *IEEE Access*, vol. 4, pp. 6250–6260, 2016.
[30] A. Celik, R. M. Radaydeh, F. S. Al-Qahtani, and M.-S. Alouini, "Resource allocation and interference management for D2D-enabled DL/UL decoupled Het-Nets," *IEEE Access*, vol. 5, pp. 22735–22749, 2017.
[31] F. Muhammad, Z. H. Abbas, and F. Y. Li, "Cell association with load balancing in nonuniform heterogeneous cellular networks: Coverage probability and rate analysis," *IEEE Trans. Veh. Technol.*, vol. 66, no. 6, pp. 5241–5255, Jun. 2017.
[32] A. Ijaz, S. A. Hassan, S. A. R. Zaidi, D. N. K. Jayakody, and S. M. H. Zaidi, "Coverage and rate analysis for downlink HetNets using modified reverse frequency allocation scheme," *IEEE Access*, vol. 5, pp. 2489–2502, 2017.
[33] A. Mahbas, H. Zhu, and J. Wang, "Unsynchronized small cells with a dynamic TDD system in a two-tier HetNet," in *Proc. IEEE 83rd Veh. Technol. Conf. (VTC Spring)*, May 2016, pp. 1–6.
[34] H. Song, X. Fang, L. Yan, and Y. Fang, "Control/user plane decoupled architecture utilizing unlicensed bands in LTE systems," *IEEE Wireless Commun.*, vol. 24, no. 5, pp. 132–142, Oct. 2017.
[35] W. Liu, S. Jin, C.-K. Wen, M. Matthaiou, and X. You, "A tractable approach to uplink spectral efficiency of two-tier massive MIMO cellular HetNets," *IEEE Commun. Lett.*, vol. 20, no. 2, pp. 348–351, Feb. 2016.
[36] H. ElSawy and E. Hossain, "Two-tier HetNets with cognitive femtocells: Downlink performance modeling and analysis in a multichannel environment," *IEEE Trans. Mobile Comput.*, vol. 13, no. 3, pp. 649–663, Mar. 2014.
[37] C. W. Tan, "Optimal power control in Rayleigh-fading heterogeneous wireless networks," *IEEE/ACM Trans. Netw.*, vol. 24, no. 2, pp. 940–953, Apr. 2016.
[38] B. Błaszczyszyn, M. Haenggi, P. Keeler, and S. Mukherjee, *Stochastic Geometry Analysis of Cellular Networks*. Cambridge, U.K.: Cambridge Univ. Press, 2018.
[39] R. Hernandez-Aquino, S. A. R. Zaidi, D. McLernon, and M. Ghogho, "Modelling and performance evaluation of non-uniform two-tier cellular networks through stienen model," in *Proc. IEEE Int. Conf. Commun. (ICC)*, May 2016, pp. 1–6.
[40] R. Hernandez-Aquino, S. A. R. Zaidi, M. Ghogho, D. McLernon, and A. Swami, "Stochastic geometric modeling and analysis of non-uniform two-tier networks: A Stienen's model-based approach," *IEEE Trans. Wireless Commun.*, vol. 16, no. 6, pp. 3476–3491, Jun. 2017.

MUHAMMAD SAJID HAROON (Graduate Student Member, IEEE) received the B.Sc. degree in electronics engineering from International Islamic University Islamabad, Pakistan, in 2007, and the M.S. degree in electrical engineering from the COMSATS Institute of Information Technology, Attock, Pakistan, in 2013. He is currently pursuing the Ph.D. degree with the Ghulam Ishaq Khan Institute of Engineering Sciences and Technology, Swabi, Pakistan, with a focus on interference management in next generation cellular networks using tools from stochastic geometry, point process theory, and spatial statistics. His research interests include interference mitigation in cellular networks, next generations cellular networks, stochastic processes, and digital signal processing.

FAZAL MUHAMMAD received the B.Sc. and M.Sc. degrees in electrical engineering from the University of Engineering and Technology, Peshawar, Pakistan, in 2004 and 2007, respectively, and the Ph.D. degree in electronic engineering from the Ghulam Ishaq Khan (GIK) Institute of Engineering Sciences and Technology, Pakistan, in 2017. He is currently working as an Assistant Professor and the Head of the Department of Electrical Engineering, City University of Science and Information Technology, Peshawar. He is the Secretary of the Peshawar Center, The Institutions of Engineers, Pakistan. His research interests include heterogeneous cellular networks, cognitive radio networks, and optical networks.

GHULAM ABBAS (Senior Member, IEEE) received the B.S. degree in computer science from the University of Peshawar, Pakistan, in 2003, and the M.S. degree in distributed systems and the Ph.D. degree in computer networks from the University of Liverpool, U.K., in 2005 and 2010, respectively. From 2006 to 2010, he was Research Associate with Liverpool Hope University, U.K., where he was associated with the Intelligent and Distributed Systems Laboratory. Since 2011, he has been with the Faculty of Computer Sciences and Engineering, Ghulam Ishaq Khan (GIK) Institute of Engineering Sciences and Technology, Pakistan. He is currently working as an Associate Professor and the Director of Huawei Network Academy. He is a Co-Founding Member of the Telecommunications and Networking (TeleCoN) Research Laboratory, GIK Institute of Engineering Sciences and Technology. His research interests include computer networks and wireless and mobile communications. He is a Fellow of The Institute of Science and Technology, U.K., and the British Computer Society.

ZIAUL HAQ ABBAS received the M.Phil. degree in electronics from Quaid-e-Azam University, Pakistan, in 2001, and the Ph.D. degree from the Agder Mobility Laboratory, Department of Information and Communication Technology, University of Agder, Norway, in 2012. In 2012, he was a Visiting Researcher with the Department of Electrical and Computer Engineering, University of Minnesota, USA. He is currently an Associate Professor with the Faculty of Electrical Engineering and a Co-Founding Member of the Telecommunications and Networking (TeleCoN) Research Laboratory, Ghulam Ishaq Khan Institute of Engineering Sciences and Technology. His research interests include energy efficiency in hybrid mobile and wireless communications networks, 4G and beyond mobile systems, mesh and *ad hoc* networks, traffic engineering in wireless networks, performance evaluation of communications protocols and networks by analysis and simulation, quality-of-service in wireless networks, green wireless communications, and cognitive radio.

AHMAD KAMAL HASSAN received the B.Eng. degree (Hons.) in electrical and electronics engineering from the University of Bradford, U.K., in 2007, the M.S. degree in electrical engineering from Karlstad University, Sweden, in 2012, and the Ph.D. degree in electrical engineering from King Abdulaziz University, Jeddah, Saudi Arabia, in 2017. He was a Consultant for radio access networks with Nokia Siemens Networks, Ericsson AB, and Advance Communication and Electronics Systems in western region of Saudi Arabia, from 2007 to 2010. He was a Research Associate with the Ghulam Ishaq Khan Institute of Engineering Sciences and Technology, from 2013 to 2014, where he has been an Assistant Professor, since 2017. He was associated with the Center of Excellence in Intelligent Engineering Systems, King Abdulaziz University. His research interests include reliability modeling and analysis of networks in general, and system modeling, performance analysis, and beamforming design of MIMO communication networks in particular. He is a Chartered Engineer (C.Eng.) and a member of the Institution of Engineering and Technology.

MUHAMMAD WAQAS received the B.Sc. and M.Sc. degrees from the Department of Electrical Engineering, University of Engineering and Technology, Peshawar, Pakistan, in 2009 and 2014, respectively, and the Ph.D. degree from the Beijing National Research Center for Information Science and Technology, Department of Electronic Engineering, Tsinghua University, Beijing, China, in 2019. He is currently serving as an Assistant Professor with the Faculty of Computer Science and Engineering, Ghulam Ishaq Khan Institute of Engineering Sciences and Technology, Pakistan. He is also Visiting Research Associate with the Beijing Key Laboratory of Trusted Computing, School of Computing, Beijing University of Technology, Beijing. He has several research publications in highly reputed journals and conferences. His current research interests include networking and communications, including 5G networks, D2D communication, resource allocation and physical layer security and information security, mobility investigation in D2D communication, fog computing, and MEC.

SUNGHWAN KIM (Member, IEEE) received the B.S., M.S., and Ph.D. degrees from Seoul National University, South Korea, in 1999, 2001, and 2005, respectively. He was a Postdoctoral Visitor with the Georgia Institute of Technology (Georgia Tech), from 2005 to 2007, and a Senior Engineer at Samsung Electronics, from 2007 to 2011. He is currently a Professor with the School of Electrical Engineering, University of Ulsan, South Korea. His main research interests include channel coding, modulation, massive MIMO, visible light communication, and quantum information.